

Multiple-type solutions for multipole interface solitons in thermal nonlinear media

Xuekai Ma, Zhenjun Yang, Daquan Lu, Wei Hu^{1,*}

¹Laboratory of Photonic Information Technology,
South China Normal University, Guangzhou 510631, P. R. China

(Dated: July 5, 2018)

We address the existence of multipole interface solitons in one-dimensional thermal nonlinear media with a step in the linear refractive index at the sample center. It is found that there exist two types of solutions for tripole and quadrupole interface solitons. The two types of interface solitons have different profiles, beam widths, mass centers, and stability regions. For a given propagation constant, only one type of interface soliton is proved to be stable, while the other type can also survive over a long distance. In addition, three types of solutions for fifth-order interface solitons are found.

PACS numbers: 42.65.Tg, 42.65.Jx

I. INTRODUCTION

Nonlocality of a nonlinear response is a property exhibited in many nonlinear optical media. Nonlocal solitons have been found in nematic liquid crystals [1–5] and lead glasses [6–9] theoretically and experimentally. They present some novel properties, for instance, the large phase shift [10], self-induced fractional Fourier transform [11], attraction between two dark solitons [12], etc. Recently, various types of nonlocal surface solitons [13–19], for example, multipole surface solitons [14, 15], vortex surface solitons [14], and incoherent surface solitons [16], have been found at the interface between a nonlinear medium and a linear medium [13–17] or between two nonlinear media [18, 19]. The surface solitons propagating at an interface formed by a nonlinear medium and a linear medium are found to be stable only when their peaks are less than three [15]. Surface solitons propagating at an interface formed by two nonlinear media are also found [18], but dipole surface solitons in such media can exist only when optical lattices exist.

Nonlocal multipole solitons are studied in nematic liquid crystals [20] and lead glass [15, 21] for both bulk solitons and surface solitons. In nonlocal bulk media, multipole solitons are symmetric, and they are stable if they contain fewer than five peaks [20, 21]. For surface multipole solitons, the profiles are asymmetric because of the existence of boundary conditions, and they are stable when the number of intensity peaks is less than three [15]. By comparison, we can qualitatively consider surface solitons as half of their corresponding solitons in bulk media [22]. For example, surface fundamental solitons can be regarded as half of dipole solitons in bulk media. However, for both bulk solitons and surface solitons in nonlocal media, only one type of solution exists in any case.

In Ref. [19], we address the existence of the fundamental and dipole interface solitons propagating at the

interface between two thermal nonlinear media with different linear refractive indices. Fundamental interface solitons are found to always be stable, and the stability of dipole interface solitons depends on the difference in linear refractive index. The boundary force effect [23] plays an important role in the stability of dipole interface solitons. It is found that the mass center of the fundamental and dipole interface solitons moves to the part with higher linear refractive index as the index difference between two media increases [19].

In this paper, we study multipole interface solitons in thermal nonlinear media. It is found that there exist two types of tripole and quadrupole interface solitons and three types of fifth-order interface solitons, respectively. The phenomenon of two (or three) soliton types is not found in other surface solitons or in bulk solitons.

II. MODEL OF INTERFACE SOLITONS

We consider a (1+1)dimensional thermal sample occupying the region $-L \leq x \leq L$. The sample is separated into two parts by the interface at $x = 0$. All parameters for the two parts are same except the linear refractive indices. The propagation of a TE polarized laser beam is governed by the dimensionless nonlinear Schrödinger equation,

(i) on the left, i.e., $-L \leq x \leq 0$,

$$i \frac{\partial q}{\partial z} + \frac{1}{2} \frac{\partial^2 q}{\partial x^2} + nq = 0, \quad \frac{\partial^2 n}{\partial x^2} = -|q|^2, \quad (1)$$

(ii) on the right, i.e., $0 \leq x \leq L$,

$$i \frac{\partial q}{\partial z} + \frac{1}{2} \frac{\partial^2 q}{\partial x^2} + nq - n_d q = 0, \quad \frac{\partial^2 n}{\partial x^2} = -|q|^2, \quad (2)$$

where x and z stand for the normalized transverse and longitudinal coordinates, q is the complex amplitude of the optical field, n is the nonlinear refractive index, and $n_d > 0$ is the difference in linear refractive index between two media. Two boundaries ($x = \pm L$) and the interface ($x = 0$) are thermally conductive. Boundary conditions

*Corresponding author's email address: huwei@scnu.edu.cn

can be described by $q(\pm L) = 0$ and $n(\pm L) = 0$, and the continuity conditions at the interface are $q(-0) = q(+0)$ and $n(-0) = n(+0)$. Thus, both q and n are continuous at the interface.

We search for soliton solutions for Eqs. (1) and (2) numerically in the form $q(x, z) = w(x) \exp(ibz)$, where $w(x)$ is a real function and b is the propagation constant. The details of the model and results for fundamental and dipole interface solitons can be found in Ref. [19]. To elucidate the stability of interface solitons, we search for the perturbed solutions for Eqs. (1) and (2) in the form $q = (w + u + iv) \exp(ibz)$, where $u(x, z)$ and $v(x, z)$ are the real and imaginary parts of the small perturbations. The perturbation can grow with a complex rate σ upon propagation. Substituting the perturbed soliton solution into Eqs. (1) and (2), one can get the linear eigenvalue problem,

$$\left. \begin{aligned} \sigma u &= -\frac{1}{2} \frac{d^2 v}{dx^2} + bv - nv, \\ \sigma v &= \frac{1}{2} \frac{d^2 u}{dx^2} - bu + nu + w \Delta n, \end{aligned} \right\} \quad (-L \leq x \leq 0), \quad (3)$$

and

$$\left. \begin{aligned} \sigma u &= -\frac{1}{2} \frac{d^2 v}{dx^2} + bv - nv + n_d v, \\ \sigma v &= \frac{1}{2} \frac{d^2 u}{dx^2} - bu + nu - n_d u + w \Delta n, \end{aligned} \right\} \quad (0 \leq x \leq L), \quad (4)$$

where $\Delta n = -2 \int_{-L}^L G(x, x') w(x') u(x') dx'$ is the refractive index perturbation, the response function $G(x, x') = (x+L)(x'-L)/(2L)$ for $x \leq x'$, and $G(x, x') = (x'+L)(x-L)/(2L)$ for $x \geq x'$ [21].

III. MULTIPOLE INTERFACE SOLITONS

The results of tripole interface solitons are shown in Fig. 1. The most interesting feature of tripole interface solitons is that there exist two different types of solutions for some given values of n_d and b . For example, when $n_d = 0.4$ and $b = 5$, two solutions are shown in Figs. 1(a) and 1(b), respectively. For the first type of solution (named type I in this paper) as shown in Fig. 1(a), two intensity peaks are located in the left part of the sample with a higher index, and one resides in the right part with a lower index. The right peak is much higher than the left two peaks because the peak of nonlinear refractive index n is located at the right side of the interface. For the type-II solution shown in Fig. 1(b), almost all three peaks are located in the left part of the sample, and the left peak is the highest. Due to the difference in the profile, the beam widths (in root-mean-square definition) for the two types of tripoles are different as shown in Fig. 1(c), and they decrease monotonically with increasing b . However, their powers, defined as $P = \int_{-L}^L |q|^2 dx$

and increasing monotonically with increasing b , are approximately equal (relative difference is smaller than 2%) as shown in Fig. 1(d).

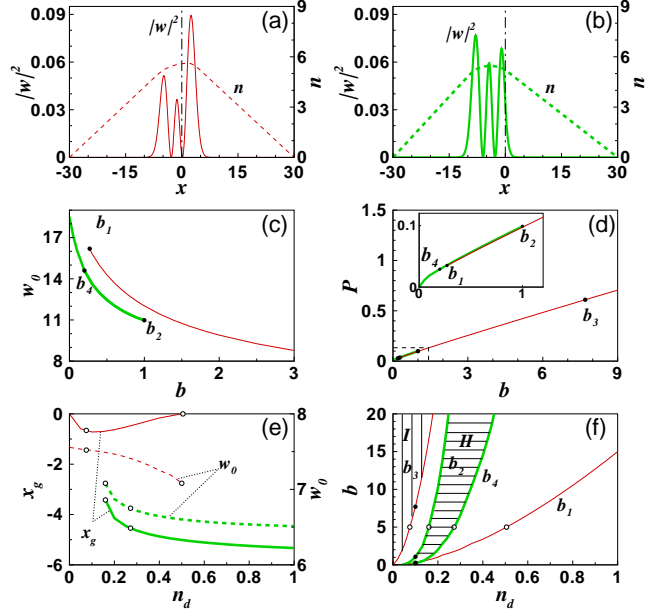


FIG. 1: (Color online) (a) and (b) Profiles for two types of tripole interface solitons at $n_d = 0.4$ and $b = 5$. Dashed-dotted lines stand for the interface. (c) Beam width versus propagation constant at $n_d = 0.1$. (d) Soliton power versus propagation constant at $n_d = 0.1$, where the inset is enlarged for small values of b . (e) Mass center and beam width versus the index difference at $b = 5$. (f) Regions of existence and stability of tripoles in the $b - n_d$ plane, where shadow areas show the stable regions. Points correspond to those cases in (c) and (d), and circles correspond to those cases in (e). Red (thin) and green (thick) lines stand for type-I and type-II tripoles, respectively, in (a)-(f).

It is known that the interface soliton in our model will reduce to the soliton in bulk media when $n_d = 0$. As n_d increases, the tripole interface soliton becomes asymmetric and shifts to the left part with a higher index. From Fig. 1(e), only the type-I tripole exists for a small value of the index difference, and its mass center (defined as $x_g = \int_{-L}^L x |q|^2 dx / P$) and center peak move into the left part as n_d increases. When n_d overtakes a certain value at a fixed b , for example, $n_d \geq 0.16$ at $b = 5$, there exist two types of tripoles [Fig. 1(f)]. It is interesting to note that the right peak of the type-I tripole always remains in the right part, and its mass center moves back to the interface as n_d increases sequentially [Figs. 1(a) and 1(e)]. For the type-II tripole, its right peak moves into the left part of the sample, and its mass center shifts toward the left and approaches a fixed value when n_d is large enough, for example, $x_g \rightarrow -6.5$ at $b = 5$ as shown in Fig. 1(e). The asymptotic feature is induced by the boundary force effect [23], and it is similar to that of fundamental and dipole interface solitons [19]. The mass

center of the type-II tripole is proportional to its beam width, whereas, the change of mass center for the type-I tripole is irrelative with its beam width [Fig. 1(e)].

The existence regions of tripole interface solitons are found numerically as $b \geq b_1$ (type I) or $b \leq b_2$ (type II) for a given index difference, where b_1 and b_2 are critical propagation constants and are given in Figs. 1(c), 1(d), and 1(f). In the overlay region ($b_1 \leq b \leq b_2$), which increases as n_d increases, shown in Fig. 1(f), two types of tripoles can exist simultaneously for a fixed n_d . For a given propagation constant, there also exists a region of n_d in which the two types of tripoles exist simultaneously. If $b = 5$, for example, the type-I tripoles exist in $n_d \leq 0.51$ and the type-II tripoles exist in $n_d \geq 0.16$, then the overlay region is $0.16 \leq n_d \leq 0.51$ [see the circle symbols in Figs. 1(e) and 1(f)].

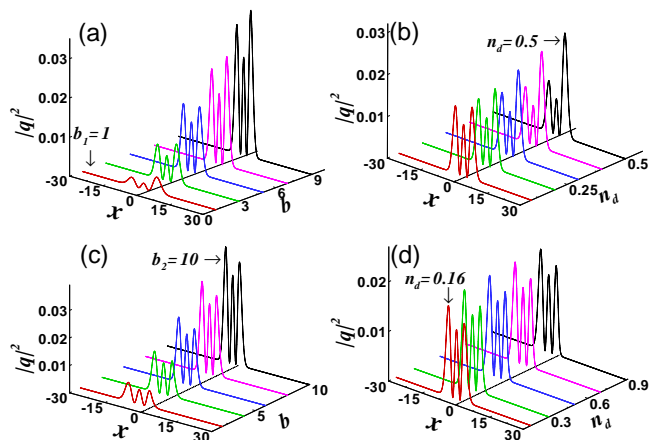


FIG. 2: (Color online) Soliton intensity profiles vary (a) with b at $n_d = 0.2$ and (b) with n_d at $b = 5$ for type-I solutions of tripole interface solitons. Soliton intensity profiles vary (c) with b at $n_d = 0.2$ and (d) with n_d at $b = 5$ for type-II solutions of tripole interface solitons.

Figure 2 shows the intensity peaks of tripole solitons vary with b and n_d for both type-I and type-II solutions. From Figs. 2(a) and 2(c), we can see that the soliton power increases with an increase in the constant propagation at a fixed n_d , which has been shown in Fig. 1(d). For a fixed n_d (for example, $n_d = 0.2$), there exist critical propagation constants for both type-I and type-II solutions as shown in Fig. 1(f). In Fig. 2(a), the critical propagation constant ($b_1 = 1$) is marked, and the type-I solution of the solitons disappears when $b < b_1$. For type-II solutions, when $b > b_2 = 10$, marked in Fig. 2(c), one cannot find this kind of solution anymore. If we fix the propagation constant, there exists critical n_d for both type-I and type-II solutions as shown in Fig. 1(f), which also can be explained by Figs. 2(b) and 2(d). Figures 2(b) and 2(d) present the change in intensity peaks versus n_d . For $n_d > 0.5$, the type-I solutions disappear [Fig. 2(b)], while one cannot find the type-II solutions for $n_d < 0.16$ [Fig. 2(d)]. It is noted that, for type-I solutions, the changes in the intensity peaks are obvious

[Fig. 2(b)], while the intensity peaks of type-II solutions change little [Fig. 2(d)].

The stability regions of tripole interface solitons are found as $b \geq b_3$ (type I) and $b_4 \leq b \leq b_2$ (type II) for a given n_d , where b_3 and b_4 are shown in Fig. 1(f). The letters I (shadow region with vertical lines) and II (shadow region with horizontal lines) in Fig. 1(f) indicate the stable zones in the $b-n_d$ plane. It is obvious that the two types of tripoles can not be stable simultaneously for a given propagation constant. In the region $b_4 \leq b \leq b_2$, the type-II tripole is stable, but the type-I tripole is not.

For comparison, tripole solitons in bulk thermal nonlinear media are stable [8, 21], but tripole surface solitons at the interface between a thermal nonlinear medium and a linear medium are unstable [15]. From Fig. 1(f), $b_1 = 0$ for type-I solutions when $n_d = 0.06$ and $b_2 = 0$ for type-II solutions when $n_d = 0.05$. Only the type-I tripoles exist for $n_d < 0.05$, and they are stable almost in their whole domain since b_3 approaches zero when n_d approaches zero. For a very large n_d , it is noted that both types of tripole interface solitons have their stability regions, unlike their counterparts in surface solitons. For the type-II tripoles, almost all the energy resides in the higher-index part, which is similar to the fundamental and dipole interface solitons [19] and surface solitons [13–15]. For the type-I tripoles, the right peak still resides in the lower-index medium even for a large n_d [Fig. 2(b)]. This unusual feature reasonably cannot be explained only by the boundary force effect, since the type-I tripole with smaller $|x_g|$ (closer to the center of the sample) should get the less equivalent force from the boundaries than the type-II tripole.

The results of quadrupole interface solitons are shown in Fig. 3, which are very similar to tripole interface solitons. There also exist two types of quadrupole interface solitons as shown in Figs. 3(a) and 3(b). The type-I quadrupole has three peaks in the left and one peak in the right, whereas, the type-II solution has four peaks in the left part. The properties of the quadrupoles are the same as that of the tripoles, except for the value of the parameters. It is worthy to note that there exist stability regions, i.e., $b \geq b_3$ (region I with vertical lines) for type-I solutions and $b_4 \leq b \leq b_2$ (region II with horizontal lines) for type-II solutions, for very large index differences. Also, we have observed that there is one peak of the type-I quadrupole still residing in the lower-index part even for a very large n_d [Fig. 3(a)].

To confirm the results of the linear stability analysis, we simulate the soliton propagation based on Eqs. (1) and (2) with the input condition $q(x, z = 0) = w(x)[1 + \rho(x)]$, where $w(x)$ is the profile of the stationary wave and $\rho(x)$ is a random function that stands for the input noise with the variance $\delta_{noise}^2 = 0.01$. Figure 4 presents propagations of tripole and quadrupole interface solitons for both type-I [Figs. 4(a), 4(c), 4(e), and 4(g)] and type-II [Figs. 4(b), 4(d), 4(f), and 4(h)]. As expected, multipole interface solitons, in their stability regions, survive over long propagation distances in the presence of the input

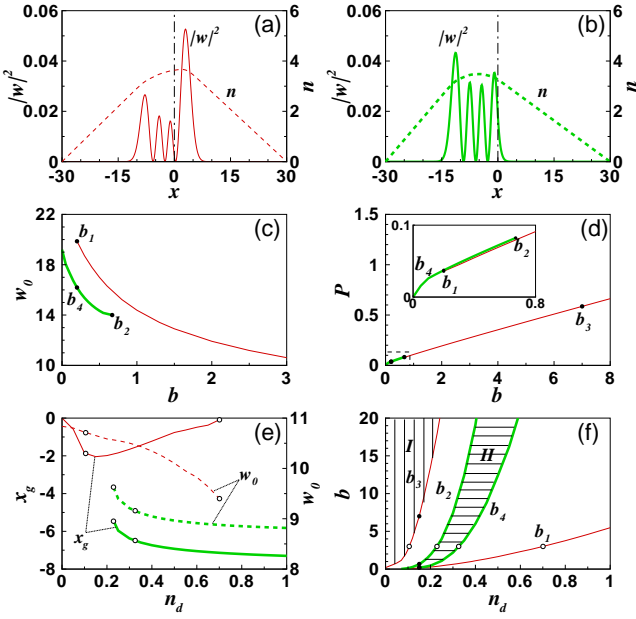


FIG. 3: (Color online) (a) and (b) Profiles for two types of quadrupole interface solitons at $n_d = 0.5$ and $b = 3$. (c) Beam width versus propagation constant at $n_d = 0.15$. (d) Soliton power versus propagation constant at $n_d = 0.15$, where the inset is enlarged for small values of b . (e) Mass center and beam width versus the index difference at $b = 3$. (f) Regions of existence and stability of quadrupoles in the $b - n_d$ plane. The style of each figure is the same as that in Fig.1.

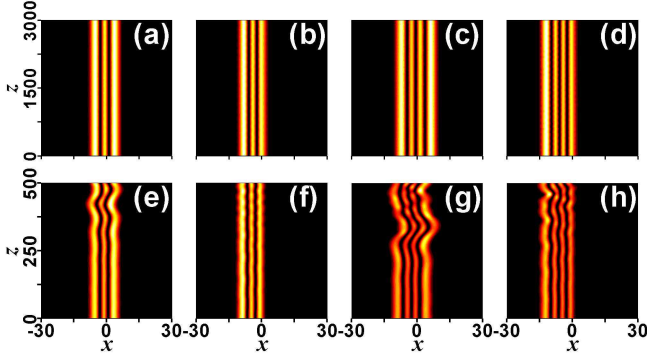


FIG. 4: (Color online) Propagations of tripole interface solitons at $b = 3$ for (a) $n_d = 0.05$, (b) $n_d = 0.15$, (e) $n_d = 0.1$, and (f) $n_d = 0.25$. Propagations of quadrupole interface solitons at $b = 2$ for (c) $n_d = 0.05$, (d) $n_d = 0.25$, (g) $n_d = 0.15$, and (h) $n_d = 0.35$.

noise (the top row). The bottom row in Fig. 4 presents propagations of multipole interface solitons in their instability regions. They experience oscillatory instability after propagating over a long distance (> 200 Rayleigh distances). This distance is long enough to observe the interface solitons in experiments, so one experimentally can observe the two types of tripole (quadrupole) interface solitons at the same n_d and b .

Figure 5 shows the results of fifth-order interface soli-

tons at different conditions. There exist three types of fifth-order interface solitons. If n_d is small, only one solution exists with three peaks on the left and two peaks on the right (type I) as shown in Fig. 5(a). When n_d increases, this type of solution disappears, and other two types of solutions exist as shown in Figs. 5(b) and 5(c). In Fig. 5(b), there are four peaks on the left and one on the right (type II), whereas, in Fig. 5(c), almost all five peaks reside on the left (type III). The existence regions of the three types of solutions for fifth-order interface solitons are shown in Fig. 5(d). The type-I solutions exist in the region $b \geq b_1$ [above the red (thin) line], and type-II solutions can be found in the region $b_2 \leq b \leq b_3$ [between the two blue (thick) lines]. At the region $b \leq b_4$ [below the green (dashed) line], one can find the type-III solutions. It is found that the number of solution types is different for different values of n_d and b [Fig. 5(d)]. For example, when $b < b_2$ or $b > b_3$, only one type of solution exists. When $n_d > 0.36$ and $b_1 < b < b_4$, three types of solutions can exist simultaneously.

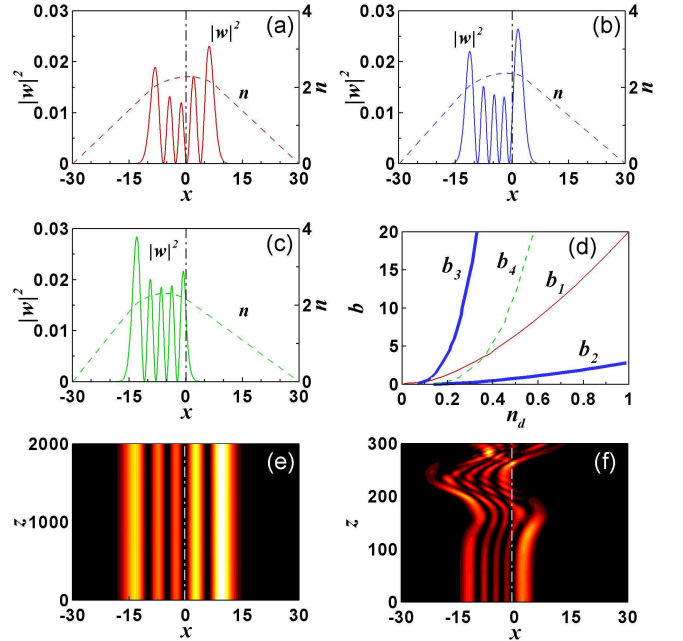


FIG. 5: (Color online) Profiles of fifth-order interface solitons at (a) $n_d = 0.2$, (b) $n_d = 0.5$, and (c) $n_d = 0.5$. For all cases $b = 3$. (d) Regions of the existence of fifth-order interface solitons in the $b - n_d$ plane. Propagations of fifth-order interface solitons at (e) $n_d = 0.129$, $b = 0.5$ and (f) $n_d = 0.5$, $b = 2$.

It is known that the solitons in bulk thermal media are unstable when the number of peaks is more than 4 [20, 21]. However, for the fifth-order interface solitons, there exists a stability region, although this region (not given here) is very small. One of the major reasons for the stable fifth-order interface solitons is the existence of the interface. For type-I solutions, one can find the stable fifth-order interface solitons when both n_d and b are small

[Fig. 5(e)]. However, there do not exist stable fifth-order interface solitons for type-II and type-III solutions. Although the two types of solutions are unstable, they can propagate a long distance as shown in Fig. 5(f). In addition, for the higher-order (more than five) interface solitons, stability regions almost do not exist.

IV. CONCLUSION

To conclude, we have studied the properties of multipole interface solitons in thermal nonlinear media. It is found that there exist two different types of tripole-quadrupole interface solitons, and three types of fifth-order interface solitons. When the linear index difference between two media is small, only the type-I solutions of the tripole and quadrupole interface solitons exist, and they are stable almost in their whole domain. When the index difference is large, two types of tripole and quadrupole interface solitons can exist stably in differ-

ent stability regions, unlike their counterparts in surface solitons. It is unusual that the right peak of the type-I multipole interface soliton still resides in the lower-index medium even for a very large n_d . In addition, our model can support stable high-order solitons with more than four peaks, which is quite different from that in uniform media, although there only exists a small stability region for the interface solitons with more than four intensity peaks. The concept mentioned in this paper can be extended to other nonlinear systems.

acknowledge

This research was supported by the National Natural Science Foundation of China (Grants No. 10804033 and No. 10674050) and the Specialized Research Fund for the Doctoral Program of Higher Education (Grant No. 200805740002).

-
- [1] M. Peccianti, K. A. Brzdakiewicz, and G. Assanto, *Opt. Lett.* **27**, 1460 (2002).
 - [2] C. Conti, M. Peccianti, and G. Assanto, *Phys. Rev. Lett.* **91**, 073901 (2003).
 - [3] C. Conti, M. Peccianti, and G. Assanto, *Phys. Rev. Lett.* **92**, 113902 (2004).
 - [4] P. D. Rasmussen, O. Bang, and W. Krolikowski, *Phys. Rev. E* **72**, 066611 (2005).
 - [5] W. Hu, T. Zhang, Q. Guo, X. Li, and S. Lan, *Appl. Phys. Lett.* **89**, 071111 (2006).
 - [6] C. Rotschild, O. Cohen, O. Manela, M. Segev, and T. Carmon, *Phys. Rev. Lett.* **95**, 213904 (2005).
 - [7] C. Rotschild, B. Alfassi, O. Cohen, and M. Segev, *Nat. Phys.* **2**, 769 (2006).
 - [8] C. Rotschild, M. Segev, Z. Xu, Y. V. Kartashov, L. Torner, and O. Cohen, *Opt. Lett.* **31**, 3312 (2006).
 - [9] S. Skupin, O. Bang, D. Edmundson, and W. Krolikowski, *Phys. Rev. E* **73**, 066603 (2006).
 - [10] Q. Guo, B. Luo, F. Yi, S. Chi, and Y. Xie, *Phys. Rev. E* **69**, 016602 (2004).
 - [11] D. Lu, W. Hu, Y. Zheng, Y. Liang, L. Cao, S. Lan, and Q. Guo, *Phys. Rev. A* **78**, 043815 (2008).
 - [12] N. I. Nikolov, D. Neshev, W. Krolikowski, O. Bang, J. J. Rasmussen, and P. L. Christiansen, *Opt. Lett.* **29**, 286 (2004).
 - [13] B. Alfassi, C. Rotschild, O. Manela, M. Segev, and D. N. Christodoulides, *Phys. Rev. Lett.* **98**, 213901 (2007).
 - [14] F. Ye, Y. V. Kartashov, and L. Torner, *Phys. Rev. A* **77**, 033829 (2008).
 - [15] Y. V. Kartashov, V. A. Vysloukh, and L. Torner, *Opt. Lett.* **34**, 283 (2009).
 - [16] B. Alfassi, C. Rotschild, and M. Segev, *Phys. Rev. A* **80**, 041808 (2009).
 - [17] Y. V. Kartashov, F. Ye, V. A. Vysloukh, and L. Torner, *Opt. Lett.* **32**, 2260 (2007).
 - [18] Y. V. Kartashov, L. Torner, and V. A. Vysloukh, *Opt. Lett.* **31**, 2595 (2006).
 - [19] X. Ma, Z. Yang, D. Lu, and W. Hu, *Phys. Rev. A* **83**, 053831 (2011).
 - [20] Z. Xu, Y. V. Kartashov, and L. Torner, *Opt. Lett.* **30**, 3171 (2005).
 - [21] L. Dong and F. Ye, *Phys. Rev. A* **81**, 013815 (2010).
 - [22] X. Ma, Z. Yang, D. Lu, Q. Guo, and W. Hu, *Phys. Rev. A* **83**, 033829 (2011).
 - [23] B. Alfassi, C. Rotschild, O. Manela, M. Segev, and D. N. Christodoulides, *Opt. Lett.* **32**, 154 (2007).